

Received January 13, 2019; reviewed; accepted June 03, 2019

## Application of sodium dodecyl glycinate to the flotation of deslimed molybdenum tailings

Yang Bai <sup>1</sup>, Caixia Li <sup>1</sup>, Wangfang Song <sup>2</sup>, Hongyun An <sup>1</sup>, Jingyu Zhao <sup>1</sup>

<sup>1</sup> College of Mining, Liaoning Technical University, Fuxin 123000, Liaoning, China

<sup>2</sup> College of Environmental Science and Engineering, Liaoning Technical University, Fuxin 123000, Liaoning, China

Corresponding author: by9211@163.com (Yang Bai)

**Abstract:** By researching the nonmetallic minerals in molybdenum tailings, this paper investigated the possible application of sodium dodecyl glycinate (SD) to deslimed tailings as an alternative to the large dosage and complex flotation reagent systems of conventional combination collectors (dodecylamine and sodium oleate). The floatability differences of nonmetallic minerals under different SD dosages were analyzed via pure mineral flotation experiments, and the adsorption behavior of SD onto different mineral surfaces was analyzed by quantum chemical calculations. The results of the calculated adsorption structures and energies of the different mineral surfaces show that SD was chemically adsorbed onto the albite (001), phlogopite (010), diopside (110), dolomite (101), calcite (104) and calcite (101) surfaces and that physical adsorption occurred at the phlogopite (001) surface. The corresponding adsorption trend was dolomite > calcite > diopside > albite > phlogopite. These results theoretically verify the feasibility of applying SD to the flotation of nonmetallic minerals in tailings and provide a basis for the selection of inhibitors needed for separating phlogopite from other minerals. In the flotation of deslimed molybdenum tailings, the recoveries of the nonmetallic minerals achieved with SD were close to those in pure mineral flotation, which was greater than the recoveries achieved with dodecylamine and sodium oleate (NaOl), and the dosage was reduced by approximately 25%.

**Keywords:** sodium dodecyl glycinate, molybdenum tailings, molecular simulation, nonmetallic minerals, amino acid collector

### 1. Introduction

The utilization of tailings is an effective way to expand the resources of raw materials and reduce the discharge amount of solid tailings, for which the economic value is no less than that of discovering one or more new ore deposits (Asokan et al., 2007). Molybdenum tailings are mainly composed of associated metallic and nonmetallic minerals. For molybdenum tailings with a low content of useful associated metallic minerals, recovering the metallic minerals alone is technologically difficult and may not be economically feasible. Therefore, the recovery of nonmetallic minerals from tailings is of great significance to improve the comprehensive utilization of resources and waste recycling (Haydn, 2000).

Currently, the multistage flotation process is usually used to recover nonmetallic minerals (mainly silicates and carbonates) from molybdenum tailings (Ren et al., 2015; Zhang et al., 2013). The commonly used collectors for silicates and carbonates are higher aliphatic acids and higher aliphatic amines, which have good collection performances but poor selectivities, low solubilities and poor hard-water resistance characteristics (Chao et al., 2007; Zhu et al., 1996). The optimum pH for flotation of these two collectors is typically in the strongly acidic range. Under neutral or near-neutral conditions, the collection ability of higher aliphatic acids and higher aliphatic amines decreases, and the reagent system is complex when these agents are used in combination (Vidyadhar et al., 2011; Majid et al., 2011). In addition, excess higher aliphatic acids and higher aliphatic amines are prone to reacting with some ions in the pulp, which not only wastes the collectors but also results in their accumulation in the circulating

water, making the flotation environment worse. Amino acid collectors have carboxyl and amine groups in their molecular structures that can react with acidic or alkaline materials to form salts. Moreover, their solubilities in acidic and alkaline environments are improved, and they can physically and chemically adsorb onto the mineral surfaces, which has a remarkable effect on mineral flotation (Jean, 2008). Among the natural amino acids, glycine is a low-cost amino acid with one carboxylic group and one amino group in its structure. In addition, glycine is a potential bidentate ligand for metal ions and possesses hydrogen-bonding sites. Metal-glycine complexes such as Cu (II), Ni (II), Ca, Mg, and Zn (II) chelates have been reported (Vimal et al., 2015; Lundager et al., 1978). Thus, a surfactant that contains a glycine fragment and hydrophobic chain might exhibit superior affinity to metal ions and function as a flotation collector for the hydrophobization of non-metallic minerals.

Over the past two decades, molecular simulations have been increasingly employed to explain and predict the interaction between collectors and minerals; molecular simulations thus provide guidance function in the design of new collectors (Guangyi et al., 2015). Numerous new collectors developed from molecular simulations have achieved good results in laboratory experiments and have been gradually applied in industrial production (Vidyadhar et al., 2011; Dianzuo et al., 2017). The present study was undertaken to explore the application of a new amino acid collector, SD, on the flotation of deslimed molybdenum tailings based on molecular simulations. Through the adsorption morphologies and adsorption energies of SD on different mineral surfaces, structure-activity relationships between the anionic dodecyl glycinate and the pure minerals were obtained, and the optimum flotation conditions were determined through flotation experiments with pure minerals and actual tailings. The SD collector developed here could potentially solve the problem of a large dosage of conventional flotation reagents and simplify the complex flotation reagent systems.

## 2. Materials and methods

### 2.1. Materials

Tailings samples in these experiments were obtained from the Xinhua molybdenum concentration plant located in Chaoyang, Liaoning Province, China. The tailing samples contained 3% moisture, and their particle size was 75.62% passing 0.074mm. The X-ray diffraction pattern shows that the tailings contain montmorillonite, which can easily be slimed and adhere to mineralized bubbles. Other nonmetallic minerals tend to be wrapped in the house-of-cards structure formed by montmorillonite, leading to a decrease in flotation selectivities and contact probabilities, which are the main causes of deterioration of the flotation environment (Wang et al., 2014). The little awl corner hydrocyclones (Gosdel & Technology Co., Ltd., Beijing, China) were selected for predesliming, being a highly precise separator and commonly used for nonmetallic mineral processing (Goog et al., 2016). The mineral composition of the deslimed molybdenum tailings was determined using a Bruker X-ray diffractometer (D8 Advance, Bruker Corp., Billerica, MA, USA), and a quantitative phase analysis was carried out using the K-value method; the results are shown in Table 1.

Table 1. The mineral composition of the deslimed molybdenum tailings

Mineral composition	Albite	Phlogopite	Diopside	Dolomite	Calcite
Content (%)	28.72	24.24	17.29	15.90	13.85

The pure minerals used in the experiment were albite and diopside from Shandong Province, China, calcite, dolomite and phlogopite from Liaoning Province, China. Fractions of 75% passing 0.074mm after crushing, grinding and classification were obtained and used for the pure mineral flotation experiments. Samples further ground to  $-5\mu\text{m}$  in an agate mortar were used for zeta potential measurements.

Chemically pure reagents were obtained from the following sources: NaOH and dodecylamine from Sinopharm Chemical Reagent Co., Ltd., Shanghai, China;  $\text{Na}_2\text{SiO}_3$ , NaOH and HCl from Shenyang Xinxing Reagents Factory, Liaoning, China. SD was synthesized following a procedure reported by Bordes and Holmberg (Romain et al., 2002).

## 2.2. Equipment

Predesliming experiments were performed on little awl corner hydrocyclones (Gosdel & Technology Co., Ltd., Beijing, China). Phase analyses of the deslimed molybdenum tailings were conducted using a Bruker X-ray diffractometer (D8 Advance, Bruker Corp., Billerica, MA, USA). Zeta potentials were measured using a Counter-Delsa440sx dynamic potential analyzer (Beckman Coulter, Inc., Brea, CA, USA). Flotation experiments were conducted in laboratory flotation machines (XFD, Jilin Exploration Machinery Corp., Changchun, China).

## 2.3. Flotation experiments

The pure mineral flotation experiments were conducted in an XFD 0.5 dm<sup>3</sup> laboratory flotation machine (XFD, Jilin Exploration Machinery Corp., Changchun, China). The main shaft speed, solids content, aeration quantity, rotor speed and bubble blowing time were kept constant at 1850 rpm, 25%, 0.25m<sup>3</sup>/(m<sup>2</sup> · min), 20rpm and 120s, respectively. The procedure used in the pure mineral flotation experiments was as follows: (1) Mineral and distilled water (pH=6.5) were added to the cell and agitated for 60s to obtain a mineral suspension. (2) The pulp pH was adjusted by adding regulators and agitating for 60s. (3) A collector and a frother were sequentially added to the slurry. The collector and frother conditioning periods were 60s and 30s, respectively. (4) The floated products were collected. (6) The concentrate products and tailings were dried at 105°C and weighed for calculation of the recovery and grade. The flowsheet of the pure-mineral flotation experiments is presented in Fig. 1.

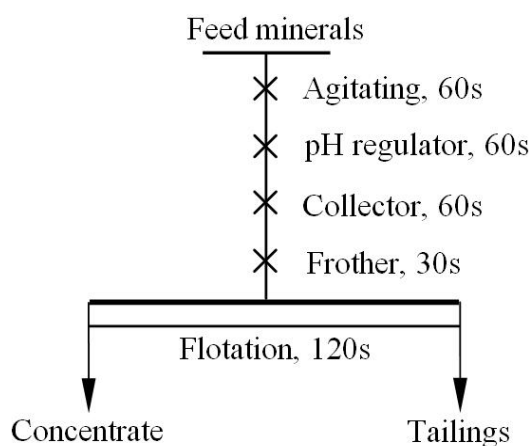


Fig. 1. The flowsheet of the pure mineral flotation experiments

## 2.4. Performance evaluation

Adsorption energies are an excellent measure of the relative intensities of the interactions between a collector and different mineral surfaces. The more negative the adsorption energy is, the more stable the system, and the more favorable the collector adsorption onto the mineral surface. In this study, the adsorption energy was used to ascertain whether different minerals can be separated by flotation. Calculations of the interaction energy were performed on configurations with the lowest energy. The adsorption energy was obtained by the following formula (Zhen et al., 2015):

$$\Delta E = E_{\text{complex}} - (E_{\text{collector}} + E_{\text{mineral}}) \quad (1)$$

where  $\Delta E$  is the adsorption energy of the collector onto the mineral surfaces and  $E_{\text{complex}}$ ,  $E_{\text{collector}}$  and  $E_{\text{mineral}}$  are the total energies of the optimized mineral surface-collector complex, collector and mineral, respectively.

All simulations were performed in Materials Studio 7.0 (MS) developed by Accelrys Inc., on a workstation. The DMol3 module included in the MS software was used to carry out the energy calculations and corresponding structure optimization to find the most stable adsorption configurations. The main parameter settings of the DMol3 module are shown in Table 2.

Table 2. The main parameter settings of the DMol3 module

Options	Parameter settings	Options	Parameter settings
Task 1	Geometry optimization	Core treatment	All electron
Task 2	Energy	Basis	DNP
Energy convergence	$1.0 \times 10^{-5}$ Ha	Max. SCF cycles	500
Displacement convergence	0.005 Å	SCF tolerance	$1.0 \times 10^{-6}$ Ha
Max. iterations	500	Max. step size	0.2 Å
Max. force	0.002 Ha/Å	Solvent	Water
Max. displacement	0.005 Å	Dielectric constant	78.54
Functional	GGA-PBE	Multipolar expansion	Hexadecapole
Symmetry	Off	Smearing	0.005 Ha
k-point (albite)	$4 \times 3 \times 3$	k-point (diopside)	$3 \times 3 \times 3$
k-point (calcite)	$3 \times 3 \times 3$	k-point (phlogopite)	$4 \times 3 \times 3$
Global orbital cutoff (albite)	4.5 Å	k-point (dolomite)	$3 \times 3 \times 3$
Global orbital cutoff (phlogopite)	4.9 Å	Global orbital cutoff (diopside)	4.8 Å
Global orbital cutoff (calcite)	4.8 Å	Global orbital cutoff (dolomite)	4.8 Å

### 3. Results and discussion

#### 3.1. Zeta potential of pure minerals

To understand the influence of the mineral surface potential on floatability, the zeta potentials of pure minerals were measured, and the results are presented in Fig. 2.

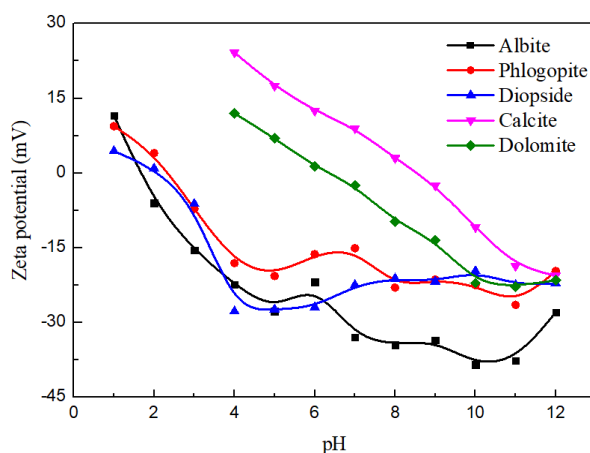


Fig. 2. The relationship between pH and zeta potentials of the pure minerals

In an aqueous solution, the point of zero charge of the silicate minerals albite, phlogopite and diopside were 1.91, 2.35 and 2.15, respectively, while that of the carbonate minerals calcite and dolomite were 8.62 and 6.25, respectively. In the flotation system, these three silicate minerals can be collected by cationic collectors under neutral conditions, which are unlikely to be selective through electrostatic forces alone. The metal coordination ions in the mineral crystals and the  $Al^{3+}$  exposed by Al-O bond fracturing provide adsorption sites for anionic collectors, in which the number and strength of the adsorption sites may be different. When the dosage of the anionic collectors is different, their flotation order may change. For carbonate minerals, cationic collectors are typically used to collect dolomite, while calcite can be collected by anionic collectors under neutral conditions. The exposed metal ions on the crystal surface provide adsorption sites for the anionic collectors. Thus, it is necessary to separate the target minerals by chemical adsorption and to control the amount of collector accurately, which is helpful to realize the selective flotation of the different target minerals.

A comparison of the results in Fig. 2 and Fig. 3 reveals that, after the interaction with SD, the zeta potential of these five non-metallic minerals shifted to more negative values, indicating that SD adsorbed onto the mineral surface in the form of anions. Moreover, the change in zeta potential on mineral surface was substantial, indicating that SD may be chemically adsorbed onto the mineral surface. The greater the change in zeta potential is, the greater the adsorption capacity of SD on the mineral surface. Within the pH range 5-7, the dolomite with adsorbed SD exhibited the largest decrease in zeta potential, followed by the calcite, phlogopite, diopside and albite. Therefore, the order of adsorption capacity of SD on the mineral surfaces is dolomite > calcite > phlogopite > diopside > albite.

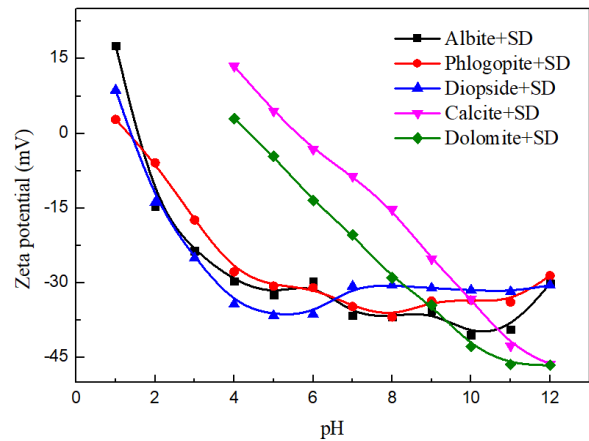


Fig. 3. The relationship between pH and zeta potentials of the pure minerals at an SD dosage of 70 mg/L

### 3.2. Pure mineral flotation experiments

The relationship between collector dosage and the recoveries of pure minerals (Fig. 4) shows that SD has good collection abilities for the pure minerals in neutral aqueous solution (pH 6.5). As the dosage of SD increased, the recoveries of different pure minerals increased gradually, from which the recoveries of calcite and dolomite were substantially affected. When the SD dosage was 60 mg/L, the recoveries of dolomite and calcite were close to 90%, and the recoveries of phlogopite and diopside were approximately 75% and 60%, respectively. Further increasing the dosage of the collector had little effect on the recoveries of these four pure minerals, but the effect on albite continued to improve. When the dosage was increased to 100mg/L, the recovery of albite stabilized at 65%. This stabilization occurred because, when the pH was 6.5, the pulp pH was close to the isoelectric point (5.97) of SD, which exists as a zwitter ion. At this point, its solubility was at its lowest, and its adsorption capacity was at its highest. Therefore, SD exhibits better collection performance on pure minerals with an increasing dosage.

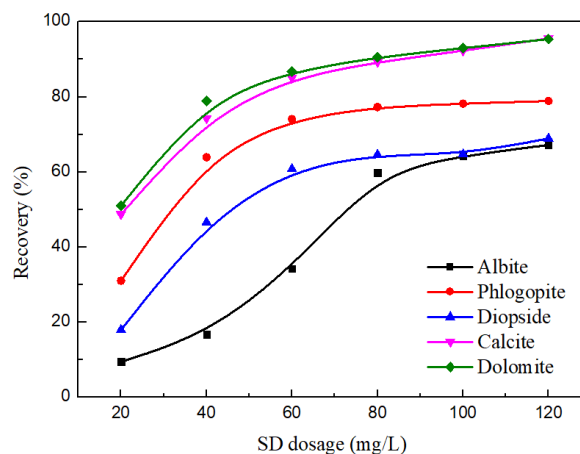


Fig. 4. The relationship between the SD dosage and the recoveries of the pure minerals

### 3.3. Flotation experiments of deslimed molybdenum tailings

Flotation experiments of deslimed molybdenum tailings were conducted in an XFD 3 dm<sup>3</sup> laboratory flotation machine; the flotation conditions were the same as those described in **Section 2.3**. Considering the relatively weak foaming performance of SD, dodecylamine at a mass fraction of 0.5% was used as a frother in the flotation experiments with SD as the collector and sodium silicate as the depressant. The specific flotation process is shown in Fig. 5, and the flotation results are shown in Table 3.

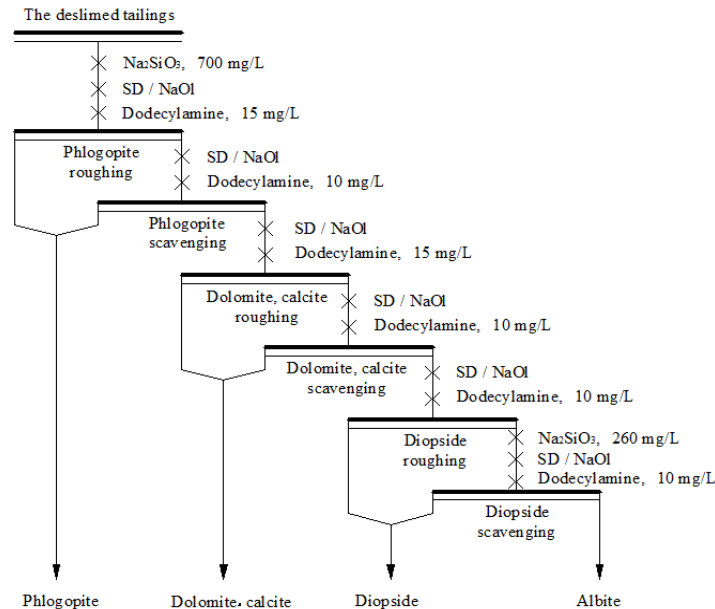


Fig. 5. The flotation process of deslimed molybdenum tailings

Table 3. Flotation indices of deslimed molybdenum tailings with different collectors

Minerals	Feeding Content* (%)	Flotation products obtained using SD			Flotation products obtained using combined collectors (NaOH, dodecylamine)		
		Collector dosage (mg/L)	Content* (%)	Recovery (%)	Collector dosage (mg/L)	Content* (%)	Recovery (%)
Phlogopite	24.24	80	17.97	74.15	120	21.13	73.09
Calcite	15.90	240	14.79	93.02	340	14.79	94.62
Dolomite	13.85	(240)	12.73	91.89	(340)	12.73	92.12
Diopside	17.29	120	11.87	68.66	130	14.95	65.56
Albite	27.82	—	17.77	63.89	—	22.04	59.95
Total	100.00	440	75.14	—	590	73.53	—

\*Accounting for the deslimed molybdenum tailings

The flotation results of deslimed molybdenum tailings (Table 3) show that the recoveries of the different nonmetallic minerals achieved with SD were close to those in pure minerals flotation, which was greater than the recoveries achieved with conventional combined collectors (dodecylamine and NaOH), and the collector dosage was reduced by approximately 25%. In the flotation of actual deslimed molybdenum tailings, it was found that if sodium silicate was not added as an inhibitor, phlogopite would float with other minerals. However, after addition, sodium silicate had obvious inhibition effect on the flotation of albite, diopside, dolomite and calcite, but poor inhibition effect on phlogopite flotation. From this it could be suggested that, the adsorption form of SD onto the phlogopite surface was different from that of other nonmetallic minerals. For further exploration of the mechanisms of SD



oxygen atom overlapped with that of the aluminum atom on the albite (001) surface. The charge of the aluminum atom increased from 1.218 to 1.372, and that of the hydroxyl oxygen atom decreased from -0.661 to -0.662, indicating that the anionic dodecyl glycinate chemisorbed onto the albite (001) surface. Meanwhile, the charge of the nitrogen atom increased from -0.463 to -0.441, and that of the carbonyl oxygen atom increased from -0.648 to -0.497. The change in the bond angles of C-N-C and O-C=O show that nitrogen atom and carbonyl oxygen atom were attracted to the albite (001) surface. However, because of their greater distance from the mineral surface, the electrostatic attraction was relatively weak.

### 3.4.3 Adsorption onto the phlogopite (001) and (010) surfaces

Phlogopite has (001) and (010) cleavage surfaces, of which the (001) surface typically exhibits perfect cleavage, and its interaction probability with a collector is greater than that of the (010) surface. The crystal structure of phlogopite was derived from the research of Pabst (Pabst, 1955). The following simulation procedures were the same as those described in Section 3.4.2 (the same below).

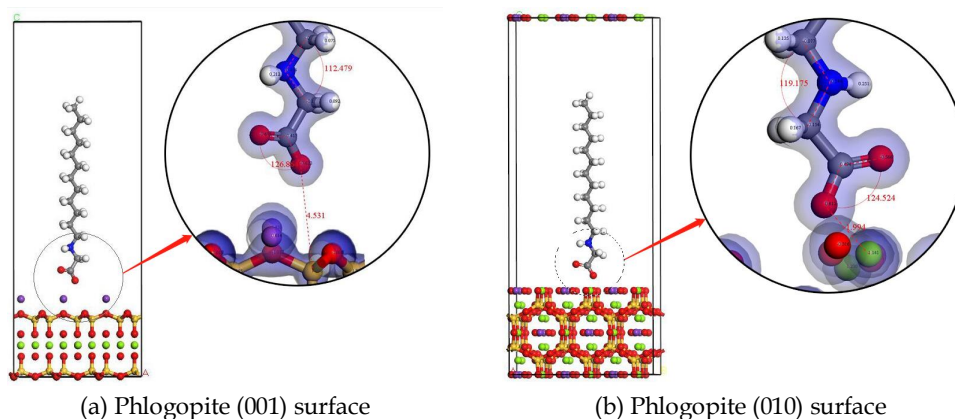


Fig. 8. The final adsorption configuration of anionic dodecyl glycinate and different phlogopite surfaces (the white, gray, blue, red, yellow, purple and green spheres represent hydrogen, carbon, nitrogen, oxygen, silicon (aluminum), potassium and magnesium, respectively)

The distance between the hydroxyl oxygen atom and the aluminum (silicon) atom increased from 2.825 Å to 4.531 Å (Fig. 8(a)), which is within the range 3.5-5.5 Å, indicating that the oxygen atoms in the same tetrahedral plane have a strong repulsive effect on the hydroxyl oxygen atom and that the interaction between the two components was the Coulomb force (Jaewook et al., 2011). The electron density of the hydroxyl oxygen atom did not overlap with that of the aluminum (silicon) atom during the whole simulation process, indicating that no chemical adsorption occurred between them. According to the charge changes, the aluminum (silicon) atom, nitrogen atom and the hydroxyl oxygen atom all showed a loss of electrons. Meanwhile, the bond angle of C-N-C decreased from 113.177° to 112.479°, and the bond angle of O-C=O slightly increased from 126.425° to 126.864°. According to the two aforementioned results, the anionic dodecyl glycinate physically adsorbed onto the phlogopite (001) surface. As shown in Fig. 8(b), anionic dodecyl glycinate adsorbed onto the magnesium atom of the phlogopite (010) surface. The charge of the magnesium atom decreased from 1.299 to 1.188 and, that of the hydroxyl oxygen atom increased from -0.661 to -0.603 after simulation. The distance (1.994 Å) between the hydroxyl oxygen and magnesium atoms is less than the sum of the ionic radii of the magnesium and oxygen atoms (2.12 Å), which proves that chemical adsorption mainly occurred on the phlogopite (010) surface. However, the cleavage of the phlogopite (010) surface was incomplete. Thus, physical adsorption of anionic dodecyl glycinate was still dominant during phlogopite collection.

### 3.4.4 Adsorption onto the diopside (110) surface

The crystal structure of diopside was derived from the research of Thompson et al. (Thompson et al., 2008). The distance between the hydroxyl oxygen atom and the magnesium atom on the diopside (110) surface, which has perfect cleavage, were shortened from 3.008 Å to 1.905 Å after simulation (Fig. 9(a)).

The electron density of the final state shows that the electron density of the hydroxyl oxygen atom did not overlap with that of the magnesium atom, indicating that they were not covalently bonded. The charge of the magnesium atom decreased from 1.308 to 1.159, while that of the hydroxyl oxygen atom increased from -0.661 to -0.502. Electron transfer occurred in the process of the hydroxyl oxygen atom approaching the magnesium atom; that is, anionic dodecyl glycinate was chemically adsorbed onto the diopside (110) surface. The bond angle of C-N-C increased from  $113.377^\circ$  to  $123.002^\circ$ , and that of O-C=O increased from  $126.425^\circ$  to  $131.230^\circ$ , indicating that the nitrogen atom and the carbonyl oxygen atom were far from the diopside (110) surface due to the repulsive forces of the oxygen atoms of the silicon-oxygen tetrahedron.

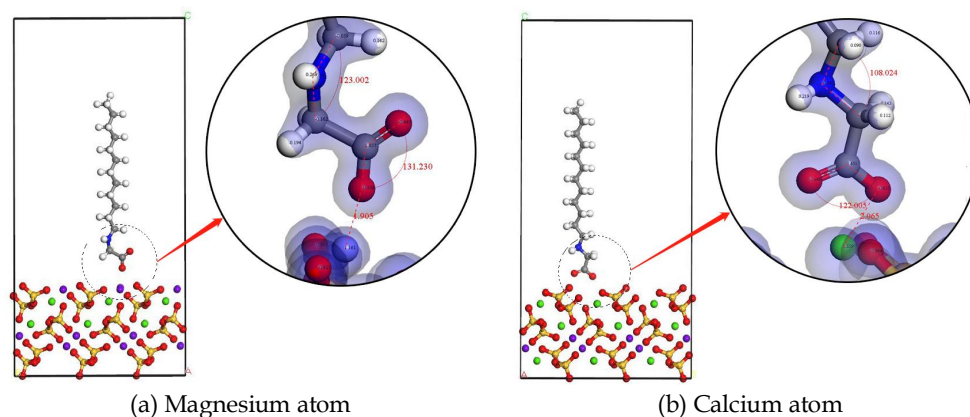


Fig. 9. The final adsorption configuration of anionic dodecyl glycinate and diopside (110) surface with different adsorption sites (the white, gray, blue, red, yellow, purple and green spheres represent hydrogen, carbon, nitrogen, oxygen, silicon (aluminum), calcium and magnesium, respectively)

However, when diopside dissociated along the (110) surface, magnesium atoms and calcium atoms were exposed with the same probability. Therefore, the adsorption process must be considered when the adsorption site is a calcium atom (Fig. 9(b)). The distance between the hydroxyl oxygen atom and the calcium atom surface was shortened after simulation (the distance was shortened from  $3.100 \text{ \AA}$  to  $2.065 \text{ \AA}$ ), as were the distances between the carbonyl oxygen atom and the nitrogen atom, which was a different result from that of the final state of the magnesium atom at the adsorption site. The decreased bond angles of C-N-C and O-C=O confirm this point (the bond angle of C-N-C increased from  $113.177^\circ$  to  $108.024^\circ$ , and that of O-C=O decreased from  $126.425^\circ$  to  $122.005^\circ$ ). The charge of the hydroxyl oxygen atom increased from -0.661 to -0.642, and that of the calcium atom decreased from 1.580 to 1.553, indicating that anionic dodecyl glycinate chemisorbed onto the diopside (001) surface.

### 3.4.5 Adsorption onto the calcite (101) and (104) surfaces

The crystal structure of calcite was derived from the research of Wyckoff (Wyckoff, 1920). The distance between the hydroxyl oxygen atom and the four calcium atoms on the calcite (101) surface changed from  $3.863 \text{ \AA}$ ,  $3.320 \text{ \AA}$ ,  $3.313 \text{ \AA}$  and  $3.883 \text{ \AA}$  to  $4.429 \text{ \AA}$ ,  $4.410 \text{ \AA}$ ,  $2.242 \text{ \AA}$  and  $3.386 \text{ \AA}$ , respectively after simulation (Fig. 10(a)). The hydroxyl oxygen atom eventually located in the area between two calcium atoms, but their electron densities did not overlap, indicating that they were not covalently bonded. The charges of the four calcium atoms changed from 0.718 to 0.697, 0.462, 1.130 and 1.150, and that of the hydroxyl oxygen atom increased from -0.661 to -0.644, which showed that electron transfer occurred during the process of the hydroxyl oxygen atom approaching the calcium atoms; that is, anionic dodecyl glycinate was chemically adsorbed onto the calcite (101) surface. The bond angle of C-N-C decreased from  $113.377^\circ$  to  $111.120^\circ$ , and that of O-C=O decreased from  $126.425^\circ$  to  $124.003^\circ$ , from which a trend of the nitrogen atom approaching the calcite (101) surface can be observed; and chemical adsorption was the main interaction between the anionic dodecyl glycinate and the calcite (101) surface.

Similar to the adsorption of anionic dodecyl glycinate onto the calcite (101) surface, the distance between the hydroxyl oxygen atom and calcium atom decreased substantially from  $2.811 \text{ \AA}$  to  $2.242 \text{ \AA}$ , and electron transfer occurred during the approach process (Fig. 10(b)). The charge of the calcium atom

decreased from 1.700 to 1.617, and that of the hydroxyl oxygen atom increased from -0.661 to -0.529, which indicates that anionic dodecyl glycinate chemically adsorbed onto the calcite (104) surface. The bond angle of C-N-C decreased from 113.377° to 112.340°, and that of O-C=O decreased from 126.425° to 125.289°, proving that the nitrogen and carbonyl oxygen atoms did not significantly approach the calcite (104) surface. Physical adsorption was not obvious.

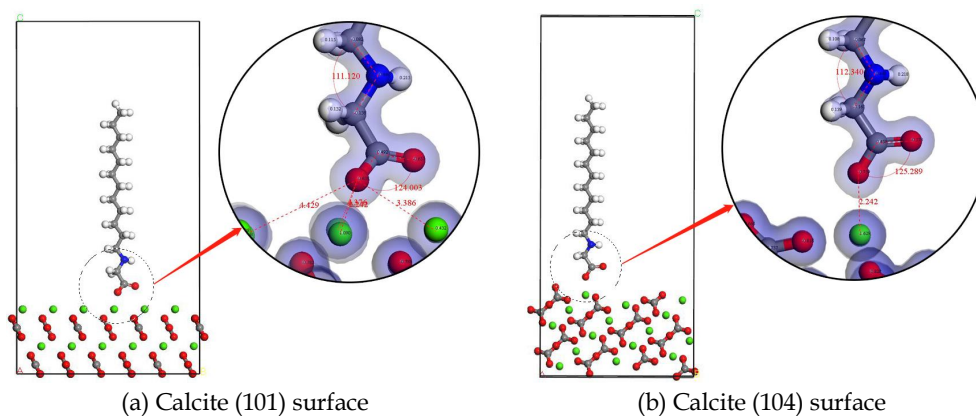


Fig. 10. The final adsorption configuration of anionic dodecyl glycinate and different calcite surfaces (the white, gray, blue, red and green spheres represent hydrogen, carbon, nitrogen, oxygen and calcium, respectively)

### 3.4.6 Adsorption onto the dolomite (101) surface

The crystal structure of dolomite was derived from the research of Steinfink (Steinfink., 1959). Dolomite is a trigonal carbonate mineral with adsorption sites of calcium and magnesium atoms. First, the adsorption at calcium atoms was considered. As seen in Fig. 11(a), the distance between the hydroxyl oxygen atom and the calcium atom decreased substantially from 2.475 Å to 2.209 Å after simulation, which is smaller than the sum of the ionic radii (2.39 Å) of the calcium atom and the oxygen atom. The charge of the calcium atom decreased from 1.798 to 1.584, while that of the hydroxyl oxygen atom increased from -0.661 to -0.556. Electron transfer occurred during the approach process, indicating that chemical adsorption of anionic dodecyl glycinate onto the dolomite (101) surface occurred. The bond angle of C-N-C decreased slightly from 113.377° to 112.031°, and that of O-C=O decreased slightly from 126.425° to 125.387°, proving that the electrostatic adsorption of the nitrogen atom and the carbonyl oxygen atom was not obvious.

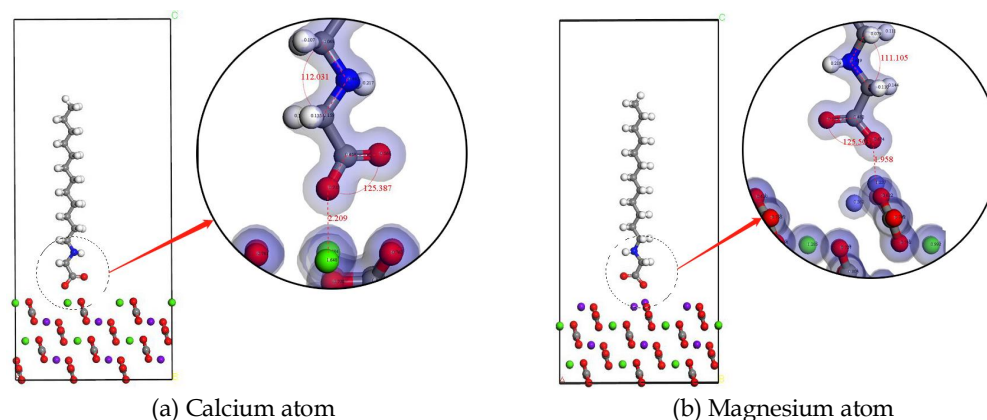


Fig. 11. The final adsorption configuration of anionic dodecyl glycinate and dolomite (101) surface with different adsorption sites (the white, gray, blue, red, purple and green beads represent hydrogen, carbon, nitrogen, oxygen, magnesium and calcium, respectively)

The adsorption conditions were similar to those of the calcium atom when the magnesium atom was the adsorption site. The distance between the carboxyl oxygen atom and the magnesium atom decreased from 3.336 Å to 1.958 Å after simulation (Fig. 11(b)). The magnesium atom lost electrons, and its charge

changed from 0.730 to 1.250. The hydroxyl oxygen atom gained electrons, and its charge changed from -0.661 to -0.685, indicating that chemical adsorption occurred during the approach process. The change in the bond angles of C-N-C and O-C=O further indicates weak electrostatic adsorption between the anionic dodecyl glycinate and the dolomite (101) surface.

### 3.4.7 Analysis of the adsorption energies for the different mineral surfaces

The adsorption energies of anionic dodecyl glycinate onto the different mineral surfaces were calculated, as shown in Table 4. The adsorption energies of anionic dodecyl glycinate on these mineral surfaces were all negative, indicating that anionic dodecyl glycinate can be adsorbed spontaneously onto the different mineral surfaces; the corresponding adsorption order was dolomite > calcite > diopside > albite > phlogopite, consistent with the flotation results of pure minerals and deslimed molybdenum tailings. The phlogopite (001) surface exhibited the adsorption energy among the investigated samples, which agreed with the results that anionic dodecyl glycinate was physically adsorbed onto the phlogopite (001) surface. This feature provides a basis for the selection of inhibitors needed for the separation of phlogopite from other minerals, and theoretically verifies the feasibility of applying SD to the flotation of nonmetallic minerals in tailings.

Table 4. The adsorption energies of anionic dodecyl glycinate onto the different mineral surfaces

Mineral surface	Adsorption site	$\Delta E$ (kJ/mol)	Average $\Delta E^*$ (kJ/mol)
Albite (001) surface	Aluminum	-584.65	-584.65
Phlogopite (001) surface	Aluminum	-92.11	-92.11**
Phlogopite (010) surface	Magnesium	-639.61	
Diopside (110) surface	Magnesium	-656.11	-668.91**
Diopside (110) surface	Calcium	-681.71	
Calcite (101) surface	Calcium	-740.83	-752.94
Calcite (104) surface	Calcium	-765.05	
Dolomite (101) surface	Calcium	-755.06	-764.06
Dolomite (101) surface	Magnesium	-773.06	

\* The probability of exposing different adsorption sites is equal when the mineral surface is cleaved.

\*\* The average  $\Delta E$  is the  $\Delta E$  of anionic dodecyl glycinate onto the phlogopite (001) surface.

## 4. Conclusions

The SD has been proven to be an efficient collector for flotation of deslimed molybdenum tailings. In the flotation of actual tailings, the recoveries of the different nonmetallic minerals were close to those in pure minerals flotation, which was greater than the recoveries achieved with conventional combined collectors (dodecylamine, NaOl), and the collector dosage was reduced by approximately 25%. Molecular simulations of SD on different mineral surfaces show that chemical adsorption can occur between the SD and the aluminum atoms of the albite (001) surface, the calcium atoms of the calcite (104) and (101) surfaces, and the calcium and magnesium atoms of the diopside (110) surface and dolomite (101) surface, while SD physically adsorbs onto the phlogopite (001) surface. According to the adsorption energies, the corresponding adsorption trend is dolomite > calcite > diopside > albite > phlogopite, consistent with the flotation results of pure minerals and deslimed molybdenum tailings. The aforementioned characteristics provide reference information for the selection of the inhibitors needed for the separation of phlogopite from other minerals and for the design of collectors for non-metallic minerals in molybdenum tailings.

## References

ASOKAN P., MOHINI S., SHYAM R., 2007. *Solid wastes generation in India and their recycling potential in building materials*. Building and Environment, 42, 2311-2320.

- CHAO L., HENGHU S., ZHONGLAI Y., LONGTU L., 2010. *Innovative methodology for comprehensive utilization of iron ore tailings Part 2: The residues after iron recovery from iron ore tailings to prepare cementitious material*. Journal of Hazardous Materials, 174, 78–83.
- DIANZUO W., 2017. *Flotation reagents: applied surface chemistry on minerals flotation and energy resources beneficiation*. Metallurgical Industry Publishing Company, Inc.
- DOWNS R., HAZEN R., FINGER L., 1994. *The high-pressure crystal chemistry of low albite and the origin of the pressure dependency of Al-Si ordering P=3.78 GPa Note: sample is from Crete*. American Mineralogist, 79, 1042–1052.
- GOOG Z., LIAO L., LV G., WANG X., 2016. *A simple method for physical purification of bentonite*. Applied Clay Science, 119, 294–300.
- GUANGYI L., XIANGLIN Y., HONG Z., 2017. *Molecular design of flotation collectors: a recent progress*. Advances in Colloid and Interface Science, 246, 181–195.
- HAYDN H., 2000. *Traditional and new applications for kaolin, smectite, and palygorskite: a general overview*. Applied Clay Science, 17, 207–221.
- JAEWOOK L., HONGJIAN Z., JAEBEOM L. 2011. *Small molecule induced self-assembly of Au nanoparticles*. Journal of Materials Chemistry, 21, 16935–16942.
- JEAN, F., 2008. *Adsorption and polymerization of amino acids on mineral surfaces: a review*. Origins of Life and Evolution of Biospheres, 38, 211–242.
- LUNDAGER H., CHRISTENSEN H., GOTTLIEB C., 1978. *Stability constants of copper (II), zinc, manganese(II), calcium, and magnesium complexes of N-(Phosphonomethyl) glycine (Glyphosate)*. Acta Chemica Scandinavica, 32, 79–83.
- MAJID E., MEHDI I., MEHDI G., 2011. *Influence of important factors on flotation of zinc oxide mineral using cationic, anionic and mixed (cationic/anionic) collectors*. Minerals Engineering, 24, 1402–1408.
- PABST A., 1955. *Redescription of the single layer structure of the micas*. American Mineralogist, 40, 967–974.
- RUICHEN R., QIANWEI Z., XIULAN W., CAIXIA L., QIANQIAN S., YUPENG F., 2015. *Experimental study on calcite and dolomite separation from molybdenum tailings*. 36,72-74.
- ROMAIN B., KRISTER H., 2001. *Physical chemical characteristics of dicarboxylic amino acid-based surfactants*. Colloids and Surfaces A: Physicochemical and Engineering Aspects, 391, 32–41.
- STEINFINK H., SANS F., 1959. *Refinement of the crystal structure of dolomite*. American Mineralogist, 44, 679–682.
- THOMPSON R., DOWNS R., 2008. *The crystal structure of diopside at pressure to 10 GPa*. American Mineralogist, 93, 177–186.
- VIDYADHAR A., NEHA K., BHAGAT R., 2011. *Adsorption mechanism of mixed collector systems on hematite flotation*. Minerals Engineering, 26, 102–104.
- VIMAL K. S., MADHU G., M. N. SRIVASTAVA, 1996. *Synthesis and characterization of complexes of copper(II), nickel(II), cobalt(II) and zinc(II) with histidine and glycine or alanine*. Synthesis and Reactivity in Inorganic and Metal-Organic Chemistry, 26, 1661-1676.
- WANG B., PENG Y., SUE V., 2014. *Effect of saline water on the flotation of fine and coarse coal particles in the presence of clay minerals*. Minerals Engineering, 66, 145–151.
- WYCKOFF R., 1920. *The crystal structure of some carbonates of the calcite group*. American Journal of Science, 50, 317–360.
- YUSHUANG Z., JIANGUANG Z., 1996. *Chemical principles of flotation reagents*. Central-South Industry University Publishing Company, Inc.
- QIANGWEI Z., RUICHEN R., CAIXIA L., 2013. *Experimental Research on Recovery of Phlogopite from Molybdenum Tailings*. Non-Metallic Mines, 38, 43-45.
- ZHEN L., ZE S., JIANGUO Y., 2015. *Investigation of dodecylammonium adsorption on mica, albite and quartz surfaces by QM/MM simulation*. Molecular Physics, 113, 3423–3430.